THE JOURNAL OF PHYSICAL CHEMISTRY B

Article

pubs.acs.org/JPCB

The Role of Multifilament Structures and Lateral Interactions in Dynamics of Cytoskeleton Proteins and Assemblies

Xin Li and Anatoly B. Kolomeisky*

Rice University, Department of Chemistry and Center for Theoretical Biological Physics, Houston, Texas 77005, United States

ABSTRACT: Microtubules and actin filaments are biopolymer molecules that are major components of cytoskeleton networks in biological cells. They play important roles in supporting fundamental cellular processes such as cell division, signaling, locomotion, and intracellular transport. In cells, cytoskeleton proteins function under nonequilibrium conditions that are powered by hydrolysis of adenosine triphosphate (ATP) or guanosine triphosphate (GTP) molecules attached to them. Although these biopolymers are critically important for all cellular processes, the mechanisms that govern their complex dynamics and force generation remain not well explained. One of the most difficult fundamental issues is to understand how different components of cytoskeleton proteins interact together. We develop an approximate theoretical approach for analyzing complex processes in cytoskeleton proteins that takes into account the multifilament structure, lateral interactions between parallel protofilaments, and the most relevant biochemical transitions during the biopolymer growth. It allows us to fully evaluate collective dynamic properties of cytoskeleton filaments as well as the effect of external forces on them. It is found that for the case of strong lateral interactions the stall force of the multifilament protein is a linear function of the number of protofilaments. However, for weak lateral interactions, deviations from the linearity are observed. We also show that stall forces, mean velocities, and dispersions are increasing functions of the lateral interactions. Physical−chemical explanations of these phenomena are presented. Our theoretical predictions are supported by extensive Monte Carlo computer simulations.

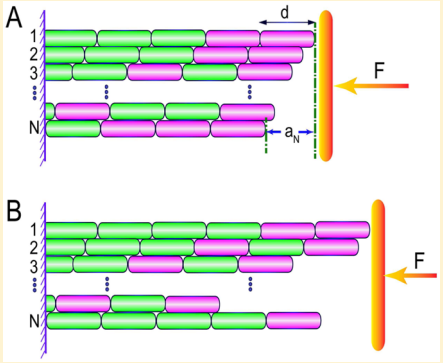

INTRODUCTION

The cytoskeleton is a complex network of filamentous proteins that supports many fundamental cellular processes such as transport of vesicles and organelles, cell division, motility, mechanical stability, and the organization of various cellular structures.[1−4] Microtubules and actin filaments are major components of the cytoskeleton systems. These biopolymers have complex structures that are important in fulfilling their cellular functions.[3,4] Microtubules are hollow cylindrical molecules typically composed of 13 parallel protofilaments, which are assembled from tubulin dimer subunits. Each tubulin dimer is capable of binding to two GTP (guanosine triphosphate) molecules, but only one of them might hydrolyze. Actin filaments, which are assembled from actin monomers, have a double-strand helical structure. Each actin monomer is associated with one ATP (adenosine triphosphate) molecule that can also hydrolyze. In biological systems, cytoskeleton filaments often form bundles and aggregates that are composed of many parallel protofilaments. The bundling apparently helps them to maintain structures with higher rigidity in order to resist larger stresses in cells.[4,5] It is also very useful for a variety of cellular processes, for example, for cell division and cell motility.

Both microtubules and actin filaments can be viewed as active polymers because they are able to fuel their dynamics with energy released from the hydrolysis of GTP or ATP molecules. During polymerization/depolymerization events, cytoskeleton proteins can produce significant forces that are crucial for many biological processes.[1−4] In recent years, dynamic properties and force generation in microtubules and actin filaments have been actively studied both experimentally and theoretically.[4−34] However, microscopic mechanisms of underlying phenomena in cytoskeleton filaments remain not well understood. The most important fundamental questions concern the relationship between structures and dynamics and how the energy of hydrolysis as well as interactions between monomers influences the force generation in microtubules, actin filaments, and cytoskeleton protein bundles.

Stimulated by strong experimental advances, several theoretical methods to uncover mechanisms of cytoskeleton filament functioning have been developed.[6−11,14−17,21,24−26,29,30,32,34] Earlier theoretical models tried to view the dynamics of cytoskeleton filaments in a very phenomenological way.[28] In a more advanced approach, the effects of the structure and interactions between biopolymer subunits on the growth dynamics and force generation in microtubules and actin filaments have been investigated.[9−11,14] However, these models cannot explain a variety of dynamic phenomena in cytoskeleton protein filaments, such as dynamic instability and large length fluctuations, because active processes of hydrolysis of ATP or GTP molecules are ignored. A different method, which takes into account the hydrolysis and

Received: February 5, 2015
Revised: March 12, 2015
Published: March 13, 2015

DOI: 10.1021/acs.jpcb.5b01219
J. Phys. Chem. B 2015, 119, 4653−4661

polymerization/depolymerization processes, is able to describe the dynamics of cytoskeleton proteins much better.[16,17,21,24,29,30] Although this approach revealed important microscopic details on complex dynamics in microtubules and actin filaments, its usefulness is diminished by neglecting the structure and interactions in these biopolymers. A computational model that includes the hydrolysis and binding/unbinding chemical transitions for multifilament biopolymers has been introduced recently.[25,34] One of the exciting findings of this work is that the dynamic properties of multifilament molecules are distinct from the dynamic properties of single filaments. However, this approach neglected important structural features such as interactions between protofilaments and parallel shifts between the protofilaments. In addition, only computational results were presented, from which it was difficult to clarify the microscopic origin of the observed phenomena.

Our goal is to develop a comprehensive theoretical framework for analyzing dynamics and force generation in cytoskeleton protein filaments that would be also useful for understanding the underlying mechanisms. In our approach, we take explicitly into account the hydrolysis of ATP/GTP molecules, attachment/detachment processes for subunits at the tip of biopolymers, lateral interactions between the parallel chains, and the correct geometry of multifilament molecules. This allows us to calculate collective dynamic properties and produced forces for a wide range of parameters. For large interactions between the protofilaments, the analysis suggests that only a few biopolymer configurations are relevant. This provides a support for our approximate analytical model that we call a one-layer model. In this case, the stall force is a linear function of the number of protofilaments. It is also found that the stall forces, the mean velocities, and the dispersions grow with increasing the lateral interactions. However, for weak lateral interactions, we predict that the dynamic features of the multifilament molecules deviate from the corresponding single-filament properties. The presented theoretical method provides a convenient way for understanding the microscopic origin of these phenomena. Our theoretical calculations are also supported by extensive Monte Carlo simulations.

THEORETICAL METHODS

We investigate a model of a multifilament molecule composed of N parallel protofilaments (labeled as 1, 2, ..., and N, respectively) with one end fixed on a substrate and the other end growing against the external load F as shown in Figure 1. To be more specific, we consider the model for single microtubule filaments, although all arguments can be easily extended for arbitrary multifilament assembly. Each protofilament in our system is surrounded by two neighboring protofilaments, and to account for the cylindrical shape of microtubules, we take a periodic boundary condition in the vertical direction (see Figure 1). The neighboring protofilaments interact with each other via chemical interactions that are generally called lateral interactions.

Experimental and theoretical studies suggest that the growing end of the microtubule might have different structures, and the geometry of a biopolymer's end, to a large degree, specifies the dynamic properties of the multifilament molecule.[9,12] To clarify the mechanisms of cytoskeleton proteins, we also analyze here a simplified version of the model, which is known as the one-layer model (see Figure 1A).[9] If we define a_i (i = 1, 2, ..., 13) as the distance of the tip of the ith protofilament from the leading

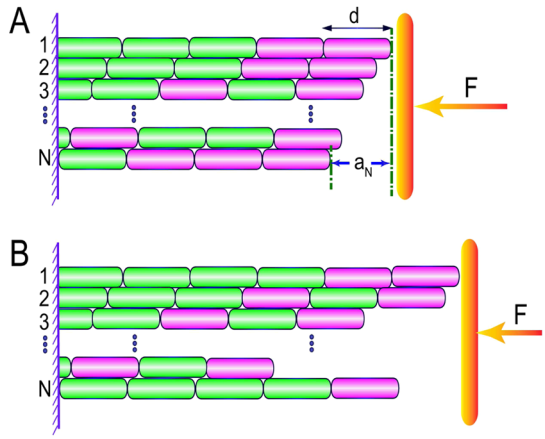

Figure 1. Theoretical models for dynamics of the multifilament assembly: (A) Approximate one-layer model, where the distances between the tip of the leading protofilament and the tips of other protofilaments are less than the size of one subunit. (B) Full dynamic model, where the distance between the tips of the leading protofilament and those of the others is not restricted. The size of one subunit is equal to d. The distance between the leading protofilament and the ith protofilament is specified by a_i with i = 1, 2, ..., 13. The external load force is given by F. Subunits bound to GTP(ATP) molecules are shown in red, while those bound to GDP(ADP) molecules are in green.

protofilament, then in the one-layer model, only configurations with $a_i \leq d$ (where $d \simeq 8.2$ nm is the size of the tubulin dimer subunit) are allowed. The physical justification for this approximation comes from the arguments that for large lateral interactions all other polymer configurations will be short-lived.[9] Only configurations with the smallest surface area of the tip structure will be important. Another advantage of using this approach is that all dynamic properties can be studied analytically. For our analysis, it will be important to compare the one-layer model (Figure 1A) with the full dynamic model (Figure 1B) where the distances between the tip of the leading protofilament and the tips of other protofilaments are not restricted at all.

Microtubules and actin filaments are assembled from GTP-tubulin dimers or from ATP-actin monomers, respectively. After the GTP/ATP-subunits are incorporated into the protofilaments, the GTP/ATP molecules might hydrolyze, transforming into GDP/ADP and phosphate (Pi) through GTP/ATP cleavage process. Then, the phosphate will be released from the subunits, leaving GDP/ADP subunits in the protofilaments. For both GTP and ATP hydrolysis in microtubules and actin filaments, the phosphate release process is the rate-limiting step.[1,2] To simplify calculations, we will treat the GTP and GDP-Pi (or ATP and ADP-Pi) as the same chemical species[15−17] by considering only the phosphate release step during the hydrolysis. As a result, each subunit in the protofilaments can be found in one of two chemical states, GTP/ATP (T) state or GDP/ADP (D) state, as indicated by red and green colors in Figure 1, respectively. The underlying mechanism of GTP/ATP hydrolysis process in microtubules and actin filaments is still not well clarified, and different hydrolysis models have been proposed and debated.[16,18−21,23,24,27−31] However, the latest study for microtubules[16] suggests that a vectorial model, which postulates that the hydrolysis can only occur at the boundary of T-subunits and D-subunits, is unrealistic. Here, we will assume a random

DOI: 10.1021/acs.jpcb.5b01219
J. Phys. Chem. B 2015, 119, 4653−4661

mechanism for GTP/ATP hydrolysis, which argues that all GTP/ATP molecules within protofilaments can be hydrolyzed with the same rate. This picture is also supported by experimental observations on microtubules.[22]

The microtubule can grow by adding free tubulin subunits from the surrounding solution. The attachment rate to the tip of the protofilament j is equal to U_j. The detachment rate of the end subunit of the protofilament j is given by $W_{j,\mathrm{T}}$ or $W_{j,\mathrm{D}}$ depending on the subunit staying in either T or D states, respectively. We assume that the multifilament assembly is in the solution with a constant concentration C_T of free T-subunits. Both attachment and detachment rates of end subunits are influenced by the presence of lateral interactions between the protofilaments. The following relation based on the detailed balance arguments can be written

$$\frac{U_j}{W_j} = \frac{U_j^0}{W_j^0} e^{\Sigma_0 |\Delta d_j|/(k_\mathrm{B} T d)} \tag{1}$$

where $\Sigma_0 \geq 0$ is the lateral interaction energy per subunit length, Δd_j is the added contact length with neighboring protofilaments after the attachment of the new subunit to the protofilament j, U_j^0 and W_j^0 are attachment and detachment rates, respectively, to the protofilaments that are not influenced by the lateral interactions (when $\Sigma_0 = 0$), T is the temperature, and k_B is the Boltzmann constant. The rate W_j in eq 1 can be $W_{j,\mathrm{T}}$ or $W_{j,\mathrm{D}}$ depending on the chemical state of the subunit at the tip of the protofilament.

The growth of the multifilament molecule exerts a force that can push or pull obstacles, which is essential for many biological processes. The external force F acts only on the leading protofilament when the multifilament biopolymer grows against a load such as a hard wall shown in Figure 1. A mechanical work $F(d - a_j)$ can be produced after one subunit is incorporated into one protofilament j if $a_j < d$. Recall that d is the size of the subunit and a_j is the distance between tips of the protofilament j and the leading protofilament. Because of the produced work, the attachment and detachment rates can be further modified as follows

$$\frac{U_j}{W_j} = \frac{U_j^0}{W_j^0} e^{[\Sigma_0 |\Delta d_j|/d - F(d-a_j)]/k_\mathrm{B} T} \tag{2}$$

Then, we can separate the attachment and detachment rates from the above equation by introducing a load distribution factor Θ and a lateral energy distribution factor θ producing

$$\begin{aligned} U_j &= U_j^0 e^{[\theta \Sigma_0 |\Delta d_j|/d - \Theta F(d-a_j)]/k_\mathrm{B} T} \\ W_j &= W_j^0 e^{[(\theta-1)\Sigma_0 |\Delta d_j|/d + (1-\Theta) F(d-a_j)]/k_\mathrm{B} T} \end{aligned} \tag{3}$$

In this article, to simplify mathematical expressions, we choose the same load distribution factor Θ, $0 \leq \Theta \leq 1$, and the same lateral energy distribution factor θ, $0 \leq \theta \leq 1$, for all protofilaments (but generally $\Theta \neq \theta$). For the case of $\Theta = 1$ and $\theta = 1$, only the attachment rates are influenced by the external load and the lateral interactions, while only the detachment rates will be affected with $\Theta = 0$ and $\theta = 0$. Thus, varying these parameters is a convenient way of quantifying the effects of the lateral interactions and external forces.

RESULTS AND DISCUSSION

One-Layer Model. We first consider the one-layer model for the growth of the multifilament molecule composed of N protofilaments as shown in Figure 1A. In this model, the distance between tips of the leading protofilament and any other protofilament is less than the size of one subunit during the whole assembly process. Therefore, a new subunit can only attach to the protofilament which is the furthest away from the tip of the leading protofilament. Then, this protofilament becomes the leading one, and the system evolves from one configuration to another. Other $N - 1$ protofilaments will become leading protofilaments successively during the addition of the next $N - 1$ subunits, and the system returns to the original configuration with the same biopolymer's end structure after binding of total N subunits. At the same time, the length of the polymer increases by the size of one subunit d. Similarly, a subunit can only detach from the leading protofilament to satisfy the one-layer model constraint, and the system reaches the original configuration after detachment of N subunits successively. However, in this case, the length of the polymer decreases by d. These arguments suggest that there are N distinct polymer configurations in the one-layer model that are connected by sequential chemical transitions of attachment and detachment of subunits.

The one-layer model has been investigated by one of us for passive biopolymers without GTP/ATP hydrolysis by mapping the assembly process of the multifilament molecule into a one-dimensional random walk on periodic lattices.[9] This method allowed us to compute explicitly all dynamic properties and the exerted forces. It was shown that the mean velocity V of the growing multifilament is given by

$$V = \frac{d}{Q_N}\left(1 - \prod_{j=1}^{N} \frac{W_j}{U_j}\right) \tag{4}$$

where the coefficient Q_N is equal to

$$Q_N = \sum_{j=1}^{N} q_j, \qquad q_j = \frac{1}{U_j}\left(1 + \sum_{k=1}^{N} \prod_{i=1}^{k} \frac{W_{j+i}}{U_{j+i}}\right) \tag{5}$$

The rates U_j, W_j are given by eq 3 for the protofilament j. The periodic boundary conditions $U_{j\pm N} = U_j$ and $W_{j\pm N} = W_j$ are also applied to the equation above.

For active filaments with ATP/GTP hydrolysis, the number N of the relevant polymer's end configurations does not change. However, the chemical composition of end subunits fluctuates between T and D states. This suggests that eq 4 applies also for active biopolymers. The attachment rate is not affected. However, the detachment rates should be modified to reflect the chemical variations. In the one-layer model, the dissociation of subunits only occurs from the leading protofilament. We define $P_{j,\mathrm{T}}$ and $P_{j,\mathrm{D}}$ as the probabilities for the tip subunit of the leading protofilament j to be in T or D state, respectively. These probabilities are normalized with $P_{j,\mathrm{T}} + P_{j,\mathrm{D}} = 1$ for $1 \leq j \leq N$. One can introduce then an effective detachment rate $W_{j,\mathrm{eff}}$ via

$$W_{j,\mathrm{eff}} = P_{j,\mathrm{T}} W_{j,\mathrm{T}} + P_{j,\mathrm{D}} W_{j,\mathrm{D}} \tag{6}$$

where $W_{j,\mathrm{T}}$ and $W_{j,\mathrm{D}}$ can also be described by eq 3 with W_j^0 replaced by $W_{j,\mathrm{T}}^0$ or $W_{j,\mathrm{D}}^0$, respectively. The rates $W_{j,\mathrm{T}}^0$ and $W_{j,\mathrm{D}}^0$ are T and D subunit detachment rates for the case of zero lateral interactions between the protofilaments and for zero

DOI: 10.1021/acs.jpcb.5b01219
J. Phys. Chem. B 2015, 119, 4653−4661

external forces. The use of a single effective detachment rate for each protofilament is an approximation. We assume here that the local chemical equilibrium between T and D states in the end subunits of each protofilament is quickly established. Obviously, there are conditions when this might not be realized. However, on the basis of extensive computer simulations (see below) for microtubules, this seems to be an excellent approximation.

Finally, employing the effective detachment rates, we obtain the mean velocity of the growing active multifilament as

$$V = \frac{d}{Q_N}\left(1 - \prod_{j=1}^{N} \frac{W_{j,\mathrm{eff}}}{U_j}\right) \tag{7}$$

where all detachment rates W_j that appeared in coefficient Q_N (see eq 5) are replaced by $W_{j,\mathrm{eff}}$. Similarly, the effective diffusion constant (dispersion) D for the growing active multifilament polymer can be written as[9]

$$D = \frac{d}{N}\left[\frac{dA_N + VB_N}{Q_N^2} - \frac{1}{2}(N+2)V\right] \tag{8}$$

where auxiliary functions A_N and B_N are expressed as

$$A_N = \sum_{j=1}^{N} U_j q_j b_j, \qquad B_j = \sum_{j=1}^{N} b_j \sum_{i=1}^{N} i q_{i+j} \tag{9}$$

with coefficients b_j given by

$$b_j = \frac{1}{U_j}\left(1 + \sum_{k=1}^{N-1} \prod_{i=1}^{k} \frac{W_{j+1-i,\mathrm{eff}}}{U_{j-i}}\right) \tag{10}$$

Another important quantity to characterize the multifilament assembly is a stall force, F_S. It is defined as opposing external load that stops the growth of the biopolymer (see Figure 1). It is also equal to the maximal force that the filament can exert. Several studies show that the stall force for a passive multifilament molecule is proportional to the number of its protofilaments.[10,32] By setting the mean velocity given by eq 7 to zero, we obtain the following relation for the stall force of the active filament:

$$\ln\left(\prod_{j=1}^{N} \frac{U_j^0}{P_{j,\mathrm{T}} W_{j,\mathrm{T}}^0 + P_{j,\mathrm{D}} W_{j,\mathrm{D}}^0}\right) = \sum_{j=1}^{N} \frac{-\Sigma_0 |\Delta d_j|/d + F_S(d - a_j)}{k_B T} \tag{11}$$

where the attachment and detachment rates given by eq 3 are utilized. The sum on the right-hand side of this equation corresponds to the energy change due to adding sequentially N subunits. Because the total contact length of N added subunits is equal to Nd and the length of the filament increases by one subunit length d, we can rewrite eq 11 as

$$\ln\left(\frac{(U^0)^N}{\prod_{j=1}^{N}(P_{j,\mathrm{T}} W_{\mathrm{T}}^0 + P_{j,\mathrm{D}} W_{\mathrm{D}}^0)}\right) = \frac{-\Sigma_0 N + F_S d}{k_B T} \tag{12}$$

Here, the rates U_j^0, $W_{j,\mathrm{T}}^0$, and $W_{j,\mathrm{D}}^0$ are constant, and they are also independent of the protofilament number j, and so the label j is omitted to simplify formulas. Finally, the expression for the stall force F_S of the active multifilament assembly yields

$$F_S = \frac{N\Sigma_0}{d} + \frac{k_B T}{d} \ln\left(\frac{(U^0)^N}{\prod_{j=1}^{N}(P_{j,\mathrm{T}} W_{\mathrm{T}}^0 + P_{j,\mathrm{D}} W_{\mathrm{D}}^0)}\right) \tag{13}$$

We can analyze this result for the case of no ATP/GTP hydrolysis in cytoskeleton filaments. For passive multifilament molecules, $P_{j,\mathrm{T}} = 1$ and $P_{j,\mathrm{D}} = 0$, and the formula simplifies into

$$F_S = \frac{N}{d}\left[\Sigma_0 + k_B T \ln\left(\frac{U^0}{W_{\mathrm{T}}^0}\right)\right] \tag{14}$$

A similar result can be obtained for active filaments with equal detachment rates $W_{\mathrm{T}}^0 = W_{\mathrm{D}}^0$. This is exactly the result obtained in previous studies.[10] The stall force for a single filament without hydrolysis is given by[33]

$$F_{S,1} = \frac{k_B T}{d} \ln\left(\frac{U^0}{W_{\mathrm{T}}^0}\right) \tag{15}$$

Comparing eqs 14 and 15 produces an important theoretical prediction that the stall force for the passive multifilament assembly composed of N noninteracting protofilaments ($\Sigma_0 = 0$) is just N times the stall force for the single passive filament with the same association and dissociation rates. However, this might not be the case for active multifilament and single-filament polymers (see eq 13) because the probabilities $P_{j,\mathrm{T}}$ and $P_{j,\mathrm{D}}$ generally depend on the end structures, and they could also have different values compared to those probabilities for the single-filament system.

Full Dynamic Model. We also investigated dynamic processes in the multifilament biopolymer by considering a full dynamic model (Figure 1 B). In this case, subunits can bind to or dissociate from any end subunits without any restrictions on possible polymer configurations. Therefore, the distance between tips of the leading protofilament and any other protofilament can attain any values as shown in Figure 1B. It is rather difficult to obtain a complete analytical description for such very complex dynamic system. However, we still can get some important approximate results under reasonable simplifications.

It has been argued that the stall force of the full dynamic model for the polymerizing microtubules and filament bundles in the absence of the hydrolysis is the same as predicted by the one-layer model.[10] These arguments can be extended to the case of active biopolymers as considered here as long as the effective detachment rates (defined in eq 6) are utilized. Thus, we derive an important conclusion that eq 13 might also serve as an approximate expression for the stall force of the active multifilament assembly in the full dynamic description. However, the exact value of the stall force for the full dynamic model is generally not the same as predicted by the one-layer model. This is because the probabilities of having end subunits in T or D states ($P_{j,\mathrm{T}}$ and $P_{j,\mathrm{D}}$) depend on the dynamics, which is different in both cases.

Stall Force of an Active Multifilament Assembly. Let us be more quantitative in evaluating the stall forces of active multifilament biopolymers. We use the microtubule molecule at specific growth conditions as an example to illustrate our approach. The relevant chemical transitions rates (detachment, attachment, and hydrolysis) for microtubules are known, and they are listed in Table 1. Also, the attachment rate U^0 depends on the concentration C_{T} of free GTP-tubulin dimers in the

DOI: 10.1021/acs.jpcb.5b01219
J. Phys. Chem. B 2015, 119, 4653−4661

Table 1. Values of Model Parameters Utilized in Calculations and the Corresponding References

parameter	rates	ref
k_{on}, the on-rate of T-tubulin dimers (plus end)	3.2 μ M^{-1} s^{-1}	2
W_T^0, the off-rate of T-tubulin dimers (plus end)	24 s^{-1}	35
W_D^0, the off-rate of D-tubulin dimer (plus end)	290 s^{-1}	2
r, the hydrolysis rate in microtubule subunits	0.2 s^{-1}	15

solution which is taken to be 100 μM. Then, the attachment rate is equal to $U^0 = k_{on}C_T = 320s^{-1}$.

As indicated by eq 14, the stall force for a passive multifilament assembly does not depend on the values of the load distribution factor Θ and the lateral energy distribution factor θ. However, those factors would influence the stall force of the active multifilament molecule by changing the probabilities $P_{j,T}$ and $P_{j,D}$. In the following calculations, we take the value $\theta = 0.5$ and vary the values of Θ between 0 and 1 as explained later. We start our analysis for the case of zero lateral interactions.

We investigate the growth dynamics of microtubules utilizing both the one-layer model and the full dynamic picture via extensive Monte Carlo computer simulations. The stall force as a function of the load distribution factor Θ is presented in Figure 2. Here, the symbols are from Monte Carlo simulations

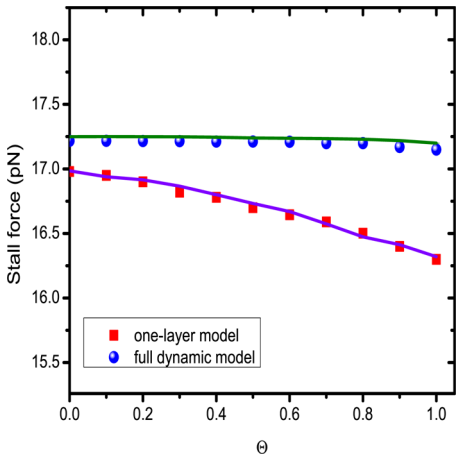

Figure 2. Stall force as a function of the load distribution factor Θ for both one-layer and full dynamic models. The lateral interaction energy Σ_0 is set to zero. The stall forces obtained from Monte Carlo simulations are indicated by red squares for the one-layer model and by blue circles for the full dynamic description. The solid lines are described by eq 13.

while the lines represent our theoretical predictions from eq 13 in which, however, we employed the values of $P_{j,T}$ and $P_{j,D}$ estimated from these computer simulations. One can see from Figure 2 that our approximate theoretical expressions for the stall forces work remarkably well.

Several interesting observations can be made by analyzing the results presented in Figure 2. First, it shows that the stall forces in the full dynamic description and in the one-layer model are a decreasing function of Θ, although the effect is much stronger for the one-layer model. This can be explained by recalling the important role of the probability to find the end subunit in the protofilament j in the T state. The larger the attachment rate U_j the higher the probability $P_{j,T}$. However, under the effect of external force F, the attachment rates are smaller as indicated by eq 3. The load distribution factor Θ specifies how the external load changes the rate U_j. For small Θ, the role of the external force is minimal while for large Θ the attachment rates decrease faster. As a result, we have a tendency to decrease $P_{j,T}$ with increasing the load distribution factor Θ. From eq 13, one might conclude then that the stall force should decrease with Θ because the detachment rate of the hydrolyzed subunits is much larger than the detachment rates of the unhydrolyzed monomers, $W_D^0 > W_T^0$ (see Table 1).

A second important observation from Figure 2 is that the stall force under the one-layer model is always smaller than the stall force for the full dynamic description, although both of them follow from the same analytical expression (see eq 13). Again, this can be explained by discussing the probabilities of having T or D end subunits on each protofilament. In the one-layer model, there is only one channel of adding T subunits to the end, while for the full dynamic model there are N channels. This leads to a higher probability to have the hydrolyzed (D) end subunit for the one-layer model, which according to eq 13 is consistent with lower stall forces. This effect is stronger for larger Θ because the external force slows down significantly the attachment rate in the one-layer model while for the full dynamic description the force has less influence on association of subunits to protofilaments that are not leading.

Recent theoretical investigations raised a question on the scaling of the stall forces as a function of the number of protofilaments.[25,34] It was shown before that the stall force of the passive multifilament molecule without lateral interactions is linearly proportional to the stall force of the single filament under the same conditions.[10] This also agrees with our theoretical predictions as indicated by eqs 14 and 15. We tested this scaling relation for active multifilament systems by employing Monte Carlo computer simulations, and the results are presented in Figure 3. Here, the ratio of the stall force for the microtubule and the stall force of the single filament times $N = 13$ is plotted for different values of the load distribution

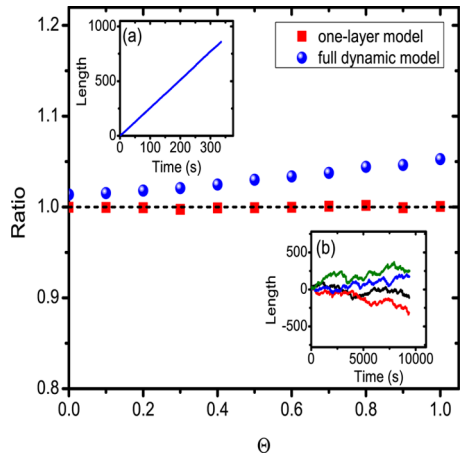

Figure 3. Ratio between the stall force for a microtubule and the stall force for a single filament times $N = 13$ as a function of the load distribution factor Θ. The ratio is shown in red squares for the one-layer model, and blue circles correspond to the full dynamic description. The dashed line indicates the ratio of the value one. Inset figures, length (in subunits) of the microtubules as a function of time (in seconds) under the force which is 13 times the stall force for a single filament for $\Theta = 1$: (a) for the full dynamic system and (b) for the one-layer model. The initial lengths of microtubules for convenience are shifted to zero.

DOI: 10.1021/acs.jpcb.5b01219
J. Phys. Chem. B 2015, 119, 4653−4661

factor Θ. If the scaling is satisfied, this ratio should be equal to one. This is the case for the one-layer model, as indicated in Figure 3, for all values of Θ. From our computer simulations of the one-layer model, we estimate that the probabilities $P_{j,T}$ and $P_{j,D}$ are almost the same for different protofilaments, and they are also very similar to the corresponding probabilities for the single filament system. This suggests that eq 13 can be rewritten in the following form:

$$F_S \approx N\frac{k_B T}{d}\ln\left(\frac{U^0}{P_T W_T^0 + P_D W_D^0}\right) \quad (16)$$

because $P_{j,T} \approx P_T$ and $P_{j,D} \approx P_D$, where P_T and P_D are the probabilities for the last subunit to be in T or D state, respectively, in the single filament model. This clearly supports the linear scaling for the multifilament biopolymers without lateral interactions under the constraint of the one-layer model, similarly to the situation with passive multifilament systems. In the inset b of Figure 3, we also present several trajectories for the assembly of microtubules under the force equal to 13 times the stall force of the single filament for Θ = 1. One can see that the lengths of the microtubules fluctuate strongly as a function of time but that the mean growth velocity averaged over many trajectories tends to be zero, validating the linear scaling arguments.

Surprisingly, the deviation from the linear scaling is observed for the full dynamic description of the system (see Figure 3), although the effect is not large (less than 5% for all values of Θ). This is closely related with the results from Figure 2. The stall force for the full dynamic description is always larger than the stall force for the one-layer model. Therefore, the ratio between the stall force of the microtubule described by the full dynamic model and 13 times the stall force of the single filament is no longer equal to one. To confirm this result, several trajectories of the microtubule assembly are also illustrated in the inset a of Figure 3 under the force of 13 times the stall force of the single filament with Θ = 1. Different from the trajectories shown in the inset b of Figure 3, the growth velocity of the microtubule or the slopes of these trajectories have positive values, supporting the deviation of the ratio of forces from being equal to one. Similar observations have been made in recent computational studies of force-dependent dynamic properties of multiple biopolymers,[25,34] although the microscopic explanations for this phenomenon were not elaborated. Our theoretical framework allows us to clarify the mechanisms of this effect. It is argued that the stall of the active multifilament assembly without lateral interactions is described by eq 13. The fact that T-subunits can attach to any protofilament in the full dynamic description leads to changes in probabilities $P_{j,T}$ and $P_{j,D}$ of finding the end subunits in T or D state, respectively. These probabilities depend on N because changing the number of protofilaments in the biopolymer modifies the associating and dissociating fluxes of tubulin subunits. Increasing N leads to larger probability for the end subunits to be in T state, which corresponds effectively to larger stall forces. This effect should be stronger for larger Θ where the influence of the external forces on attachment rates is stronger for the one-layer model than in the full dynamic picture, and our computer simulations fully support these arguments (see Figure 3).

Influence of Lateral Interactions. In our previous theoretical calculations, interactions between neighboring protofilaments have been ignored. However, real microtubules and other cytoskeleton bundles have significant lateral interactions that are important for their chemical, mechanical, and dynamic properties.[4,9,12] In the absence of lateral interactions, all polymer configurations with arbitrary distances between tips of protofilaments are equally possible. However, the lateral interactions change this picture dramatically. For the growing or shrinking multifilament assembly, the system will tend to fill gaps between the protofilaments faster, leading to more blunt tip geometries for the biopolymer's end. This suggests that only a few configurations might be responsible for dynamics of microtubules and other cytoskeleton filaments. Then, the one-layer model should be much more relevant for understanding the dynamic properties of multifilament assemblies.

For our discussions on the role of the lateral interactions, we start with the analysis of the stall forces for microtubules. In our calculations, we take the load distribution factor Θ = 1 and the lateral energy distribution factor θ = 0.5 unless otherwise specified. In Figure 4, the stall force as a function of the lateral interaction energy Σ_0 is presented for the one-layer model and for the full dynamic description. One can see that the stall forces increase with the strength of the lateral interactions, in full agreement with our theoretical predictions from eq 13. Physically, this can be understood using the following arguments. In the biopolymer with lateral interactions, adding subunits leads to larger free energy change in comparison with the case of zero lateral interactions. Then, the growing filament can produce larger work against the external load, which corresponds to the larger stall forces. In addition, we can see also in Figure 4 that the stall force for the full dynamic picture is larger than the stall force for the one-layer model (see inset in Figure 4), in agreement with our previous results from Figures 2 and 3. However, the difference is small, and it quickly disappears for large Σ_0, supporting our arguments that the one-layer model is an excellent approximation to describe the multifilament assembly with strong lateral interactions.

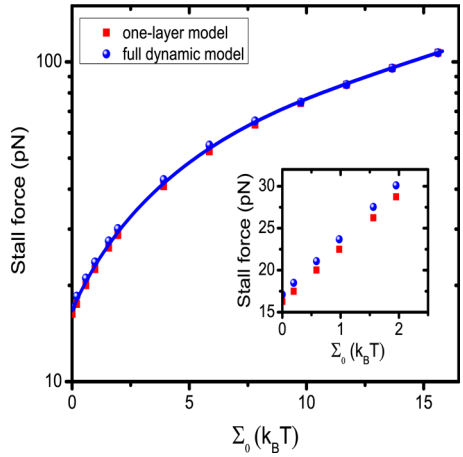

Figure 4. Stall forces of the microtubule as a function of the lateral interaction energy Σ_0. The stall forces for the one-layer model are plotted as red squares, and blue circles indicate the results for the full dynamic description. The solid line corresponds to theoretical results as explained in the text. The inset figure shows the stall forces in a regime of small lateral interaction energies.

The fact that the one-layer model works so well for description of the growth dynamics in multifilament cytoskeleton proteins with lateral interactions is crucial since

DOI: 10.1021/acs.jpcb.5b01219
J. Phys. Chem. B 2015, 119, 4653−4661

it allows us to compute explicitly all dynamic properties. It can be done by mapping the two-dimensional assembly process of the multifilament molecule into the growth of a single filament in one-dimension. As discussed previously, the stall force is not influenced by the shifts between protofilaments; therefore, the attachment and detachment rates can be written in a simpler form as

$$U = U^0 e^{[\theta\Sigma_0 - \Theta Fd/N]/k_B T}$$
$$W_T = W_T^0 e^{[(\theta-1)\Sigma_0 + (1-\Theta)Fd/N]/k_B T}$$
$$W_D = W_D^0 e^{[(\theta-1)\Sigma_0 + (1-\Theta)Fd/N]/k_B T} \quad (17)$$

In these expressions, we use the condition of the equal shifts which gives us $|\Delta d_j| = d$ and $d - a_j = d/N$. The probabilities P_T and P_D in the single filament system have been investigated before using a mean-field approach.[15] Here, we will briefly review the method.

We define an occupation number n_i for the subunit i counting from the growing tip of the filament. It is equal to 1 or 0 depending on finding the end subunit in T or D-state, respectively. Then, the master equations for the average occupation number $\langle n_i \rangle$ can be written as

$$\frac{d\langle n_i \rangle}{dt} = U\langle n_{i-1} - n_i \rangle + W_T\langle n_1(n_{i+1} - n_i)\rangle + W_D\langle (1 - n_1)(n_{i+1} - n_i)\rangle - r\langle n_i \rangle \quad (18)$$

where the random GTP hydrolysis mechanism is assumed and the transition rates are given by eq 17. The equation for the average occupation number $\langle n_1 \rangle$ of the tip subunit, which is equal to the probability P_T defined above, is given by

$$\frac{d\langle n_1 \rangle}{dt} = U\langle 1 - n_1 \rangle - W_T\langle n_1(1 - n_2)\rangle + W_D\langle (1 - n_1)n_2\rangle - r\langle n_1 \rangle \quad (19)$$

Then, we apply the mean-field arguments to the above equations, and the correlations between occupation numbers of two subunits can be neglected so that $\langle n_i n_j \rangle \approx \langle n_i \rangle \langle n_j \rangle$. At steady state, a solution $\langle n_{i+1} \rangle / \langle n_i \rangle = b$ can be obtained from the above equations where b is a constant,

$$b = \frac{U - P_T(W_T + r)}{U - P_T W_T} \quad (20)$$

The probability P_T can be obtained explicitly as a function of all transition rates which is the solution of the following cubic equation[36]

$$[U - (U + W_T + r)P_T](U - P_T W_T) + [W_T P_T + W_D(1 - P_T)][U - (W_T + r)P_T]P_T = 0 \quad (21)$$

with $0 \le P_T \le 1$. The growth velocity of the multifilament assembly described by eq 7 is simplified then as

$$V = \frac{d}{N}(U - W_T P_T - W_D P_D) \quad (22)$$

which is the same as the mean velocity of a single filament with subunit length of the size d/N. The mean velocity of the system vanishes under the stall force, that is, the left-hand side of eq 22 is equal to zero at this force. Then, combining eqs 17 and 21, the stall forces can be calculated directly for various values of the lateral interaction energy Σ_0, as indicated by the solid line in Figure 4. It clearly shows a perfect agreement with the simulation results even for the full dynamic picture, but it works especially well for the one-layer model. Therefore, the theoretical method developed for the active multifilament assembly in the one-layer model works quantitatively well, and we can apply this method to investigate other properties of the system.

Mean Velocity and Dispersion. In this section, we investigate properties of the mean growth velocity and dispersion of an active multifilament molecule under varying external forces and lateral interaction energies. For the one-layer model with equal distance shift between the protofilaments, the mean-field approach developed above can be easily utilized for evaluating all dynamic properties of the biopolymer. The probability P_T can be obtained by solving eq 21 directly given the external force F and the lateral interaction energy Σ_0. Then, the mean growth velocity and dispersion can be calculated from eqs 7 and 8, respectively. The force−velocity curve for the microtubule from Monte Carlo computer simulations and from our analytical calculations is presented in Figure 5A. In this case, the lateral interaction energy is

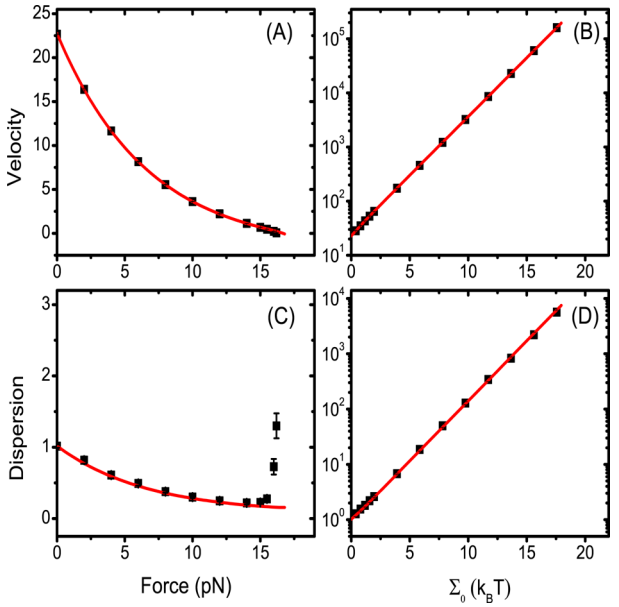

Figure 5. Mean growth velocity and dispersion of the microtubule. (A) Velocity (in subunit/s) as a function of the external force F with noninteracting protofilaments; (B) velocity as a function of the lateral interaction energy Σ_0 with zero external forces; (C) dispersion (in subunit^2/s) as a function of the external force F with noninteracting protofilaments; (D) dispersion as a function of the lateral interaction energy Σ_0 with zero external forces. Black squares are from simulations, and solid red lines are described by eqs 7 and 8 as explained in the text.

neglected. It can be seen that the mean velocity is a nonlinear decreasing function of the external force, and the theoretical predictions given by eq 7 perfectly agree with the simulation results. In a similar fashion, we can analyze the dependence of the dispersion on the external load, as shown in Figure 5C. The dispersion also decreases with increasing the external force F until the stall force, and our theoretical predictions quantitatively describe this. However, near the stall force, the system experiences significant fluctuations, leading to an

DOI: 10.1021/acs.jpcb.5b01219
J. Phys. Chem. B 2015, 119, 4653−4661

increase in dispersion. This behavior is not captured by our model because at these conditions the correlations between states of neighboring subunits become important[17] and the mean-field approximations made in eqs 18 and 19 are no longer applicable. However, in this case, one can utilize a better theoretical method that takes into account spatial correlation in the chemical composition of cytoskeleton proteins.[17]

In our approach, we can also evaluate the influence of the lateral interactions on the mean growth velocity and dispersion of the microtubule. Let us consider the case of zero external forces. The mean velocity and the dispersion as a function of the lateral interactions obtained from simulations and from our analytical calculations are shown in Figure 5B and D, respectively. Again, excellent agreement between theoretical predictions and computer simulations is found for all ranges of the lateral interactions. We determine that the mean velocity increases exponentially as the lateral interactions between protofilaments become stronger (see Figure 5B). Similar behavior is found for dispersion (Figure 5D). These observations can be easily understood if we recall that the lateral interactions exponentially modify transition rates, as indicated in eq 3.

Our main theoretical suggestion is that increasing the lateral interactions decreases the number of polymer configurations that are relevant for dynamics of multifilament molecule. In this case, the one-layer model should properly account for these changes by neglecting less important configurations. To test further these ideas, we would like to compare the velocity and dispersion of the microtubule obtained in the one-layer approximation with the full dynamic picture. The ratio for the mean velocities in two models as a function of the lateral interaction energy is presented in Figure 6A. One can see that

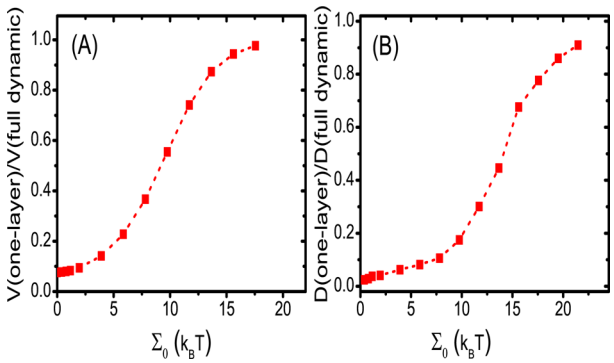

Figure 6. (A) Ratio of mean growth velocities for the one-layer and for the full dynamic picture as a function of the lateral interaction energy Σ_0. (B) Ratio of dispersions for the one-layer and for the full dynamic picture as a function of the lateral interaction energy Σ_0. Dynamic properties for the one-layer model are obtained analytically while the corresponding properties for the full dynamic description are from computer simulations.

V in the one-layer model is always smaller. This is because only attachments and detachments to specific protofilaments are allowed, while in the full dynamic model subunits can bind or unbind from all protofilaments. However, as the lateral interactions increase, the association/dissociation processes described by the one-layer model become dominant (all other rates slow down). As a result, the ratio of velocities is quickly approaching unity for $\Sigma_0 \geq 10\ k_BT$. Similar behavior is observed for dispersion as shown in Figure 6B.

The lateral interactions for microtubules have not been measured experimentally, but theoretical estimates suggest that Σ_0 is probably in the range between 3 and 10 k_BT.[9,19] It is possible that the energy is even stronger for bundles of filaments because of the larger area of interactions. This suggests that the one-layer model provides a very reasonable quantitative description of the complex processes in multifilament proteins. It also clarifies many issues associated with growth dynamics in cytoskeleton biopolymers.

SUMMARY AND CONCLUSIONS

In this article, we investigated dynamic processes in cytoskeleton proteins by explicitly taking into account the multifilament structure, the lateral interactions, and the geometry of the biopolymer ends. Our theoretical method also accounts for most relevant chemical transitions in cytoskeleton filaments such as attachment/detachment of subunits and ATP/GTP hydrolysis. It is shown that the dynamics of active biopolymers, where hydrolysis is taking place, is quite different from passive cytoskeleton filaments (without hydrolysis). In addition, the lateral interactions significantly modify the dynamic behavior of multifilament molecules.

Using theoretical arguments that only a few polymer configurations are relevant for multifilament systems with lateral interactions between subunits, we developed a theoretical framework that allows us to calculate explicitly all dynamic properties of cytoskeleton proteins. This approximate method works surprisingly well even for the case of no lateral interactions. However, the most important advantage of this approach is the ability to explain the microscopic foundations of complex processes in cytoskeleton filaments. All theoretical predictions are tested and fully supported by extensive computer Monte Carlo simulations.

It is found that the stall force of the one-layer model slightly underestimates the correct value of the stall force for the full dynamic system. The reason for this is that there are many possibilities for the subunit attachments in the full dynamic description, while in the one-layer model there are only a few of them. As a result, the end subunits in the full dynamic picture have a higher probability to be in the unhydrolyzed state, which leads to larger stall forces for typical conditions in microtubules. This effect is stronger when the external forces do not affect the association rates in the full dynamic description much in comparison with the one-layer model. We also investigated the scaling of the stall force as a function of the number of protofilaments. For weak lateral interactions, the expected linear scaling is observed in the one-layer model. However, the behavior is different in the full dynamic description, where the deviations from linearity, although not significant, are found. It is argued that the mechanism of this phenomenon is associated with the fact that the probability to have end subunits in T or D states depends on the number of protofilaments.

Our theoretical method is convenient for analyzing the influence of the lateral interactions on dynamics of cytoskeleton proteins. We found that the stall force, the mean growth velocity, and the dispersion are increasing functions of the lateral interactions. This is related to the fact that the lateral interactions effectively increase the attachment rates and decrease the detachment rates. Theoretical calculations indicate that the one-layer model provides a quantitative agreement with the full dynamic description for the stall forces of microtubules, and the linear scaling with the number of

DOI: 10.1021/acs.jpcb.5b01219
J. Phys. Chem. B 2015, 119, 4653−4661

protofilaments is restored for realistic values of the lateral interactions. At the same time, the mean growth velocity and dispersion asymptotically approach the correct values in the limit of large lateral interactions.

Although the presented theoretical method is approximate, the comparison between analytical calculations and extensive computer simulations suggests that our approach probably correctly captures the main physical and chemical processes responsible for complex dynamics in cytoskeleton proteins. However, our model still does not take into account many important features of microtubules and actin filaments, such as mechanical degrees of freedom and their coupling to underlying biochemical processes. It will be important to test our theoretical predictions in experimental studies as well as in the more advanced theoretical analysis.

AUTHOR INFORMATION

Corresponding Author

*Phone: +1 713 3485672. Fax: +1 713 3485155. E-mail: tolya@rice.edu.

Notes

The authors declare no competing financial interest.

ACKNOWLEDGMENTS

The work was supported by grants from the Welch Foundation (C-1559) and the NSF (Grant CHE-1360979) and by the Center for Theoretical Biological Physics sponsored by the NSF (Grant PHY-1427654).

REFERENCES

(1) Alberts, B., Johnson, A., Lewis, J., Raff, M., Roberts, K., Walter, P. *Molecular Biology of the Cell*, 5th ed.; Garland Science: New York, 2007.

(2) Howard, J. *Mechanics of Motor Proteins and the Cytoskeleton*; Sinauer Associates: Sunderland, MA, 2001.

(3) Desai, A.; Mitchison, T. J. Microtubule Polymerization Dynamics. *Annu. Rev. Cell Dev. Biol.* **1997**, *13*, 87−117.

(4) Huber, F.; Schnaus, J.; Ronicke, S.; Rauch, P.; Muller, K.; Futterer, C.; Kas, J. Emergent Complexity of the Cytoskeleton: From Single Filaments to Tissue. *Adv. Phys.* **2013**, *62*, 1−112.

(5) Bray, D. *Cell Movements: From Molecules to Motility*; 2nd ed.; Garland Publishing: New York, 2001.

(6) Peskin, C. S.; Odell, G. M.; Oster, G. F. Cellular Motions and Thermal Fluctuations: the Brownian Ratchet. *Biophys. J.* **1993**, *65*, 316−324.

(7) Mogilner, A.; Oster, G. The Polymerization Ratchet Model Explains the Force-Velocity Relation for Growing Microtubules. *Eur. Biophys. J.* **1999**, *28*, 235−242.

(8) Ranjith, P.; Lacoste, D.; Mallick, K.; Joanny, J. F. Nonequilibrium Self-Assembly of a Filament Coupled to ATP/GTP Hydrolysis. *Biophys. J.* **2009**, *96*, 2146−2159.

(9) Stukalin, E. B.; Kolomeisky, A. B. Simple Growth Models of Rigid Multifilament Biopolymers. *J. Chem. Phys.* **2004**, *121*, 1097−1104.

(10) Krawczyk, J.; Kierfeld, J. Stall Force of Polymerizing Microtubules and Filament Bundles. *Europhys. Lett.* **2011**, *93*, 28006.

(11) Tsekouras, K.; Lacoste, D.; Mallick, K.; Joanny, J. F. Condensation of Actin Filaments Pushing against a Barrier. *New J. Phys.* **2011**, *13*, 103032.

(12) Gardner, M. K.; Charlebois, B. D.; Janosi, I. M.; Howard, J.; Hunt, A. J.; Odde, D. J. Rapid Microtubule Self-assembly Kinetics. *Cell* **2011**, *146*, 582−592.

(13) Mahadevan, L.; Matsudaira, P. Motility Powered by Supramolecular Springs and Ratchets. *Science* **2000**, *288*, 95−99.

(14) Stukalin, E. B.; Kolomeisky, A. B. Polymerization Dynamics of Double-Stranded Biopolymers: Chemical Kinetic Approach. *J. Chem. Phys.* **2005**, *122*, 104903.

(15) Padinhateeri, R.; Kolomeisky, A. B.; Lacoste, D. Random Hydrolysis Controls the Dynamic Instability of Microtubules. *Biophys. J.* **2012**, *102*, 1274−1283.

(16) Li, X.; Kolomeisky, A. B. Theoretical Analysis of Microtubules Dynamics Using a Physical-Chemical Description of Hydrolysis. *J. Phys. Chem. B* **2013**, *117*, 9217−9223.

(17) Li, X.; Kolomeisky, A. B. A New Theoretical Approach to Analyze Complex Processes in Cytoskeleton Proteins. *J. Phys. Chem. B* **2014**, *118*, 2966−2972.

(18) Blanchoin, L.; Pollard, T. D. Hydrolysis of ATP by Polymerized Actin Depends on the Bound Divalent Cation but not Profilin. *Biochemistry* **2002**, *41*, 597−602.

(19) VanBuren, V.; Odde, D. J.; Cassimeris, L. Estimates of Lateral and Longitudinal Bond Energies within the Microtubule Lattice. *Proc. Natl. Acad. Sci. U.S.A.* **2002**, *99*, 6035−6040.

(20) Bindschadler, M.; Osborn, E. A.; Dewey, C. F.; McGrath, J. L. A Mechanistic Model of the Actin Cycle. *Biophys. J.* **2004**, *86*, 2720−2739.

(21) Vavylonis, D.; Yang, Q.; O'Shaughnessy, B. Actin Polymerization Kinetics, Cap Structure and Fluctuations. *Proc. Natl. Acad. Sci. U.S.A.* **2005**, *102*, 8543−8548.

(22) Dimitrov, A.; Quesnoit, M.; Moutel, S.; Cantaloube, I.; Pous, C.; Perez, F. Detection of GTP-Tubulin Conformation in Vivo Reveals a Role for GTP Remnants in Microtubule Rescues. *Science* **2008**, *322*, 1353−1356.

(23) Pantaloni, D.; Hill, T. L.; Carlier, M. F.; Korn, E. D. A Model for Actin Polymerization and the Kinetic Effects of ATP Hydrolysis. Procedure. *Natl. Acad. Sci. U.S.A.* **1985**, *82*, 7207−7211.

(24) Stukalin, E. B.; Kolomeisky, A. B. ATP Hydrolysis Stimulates Large Length Fluctuations in Single Actin Filaments. *Biophys. J.* **2006**, *90*, 2673−2685.

(25) Das, D.; Das, D.; Padinhateeri, R. Force-Induced Dynamical Properties of Multiple Cytoskeletal Filaments are Distinct from that of Single Filaments. *PLoS One* **2014**, *9*, e114014.

(26) Jemseena, V.; Gopalakrishnan, M. Microtibule Catastrophe from Protofilament Dynamics. *Phys. Rev. E* **2013**, *88*, 032717.

(27) Pieper, U.; Wegner, A. The End of a Polymerizing Actin Filament Contains Numerous ATP-Subunit Segments That Are Disconnected by ADP-Subunits Resulting from ATP Hydrolysis. *Biochemistry* **1996**, *35*, 4396−4402.

(28) Flyvbjerg, H.; Holy, T. E.; Leibler, S. Stochastic Dynamics of Microtubules: A Model for Caps and Catastrophes. *Phys. Rev. Lett.* **1994**, *73*, 2372−2375.

(29) Li, X.; Kierfeld, J.; Lipowsky, R. Actin Polymerization and Depolymerization Coupled to Cooperative Hydrolysis. *Phys. Rev. Lett.* **2009**, *103*, 048102.

(30) Li, X.; Lipowsky, R.; Kierfeld, J. Coupling of Actin Hydrolysis and Polymerization: Reduced Description with Two Nucleotide States. *Europhys. Lett.* **2010**, *89*, 38010.

(31) Burnett, M. M.; Carlsson, A. E. Quantitative Analysis of Approaches to Measure Cooperative Phosphate Release in Polymerized Actin. *Biophys. J.* **2012**, *103*, 2369−2378.

(32) Van Doorn, G. S.; Tanase, C.; Mulder, B. M.; Dogterom, M. On the Stall Force for Growing Microtubules. *Eur. Biophys. J.* **2000**, *29*, 2−6.

(33) Theriot, J. A. The Polymerization Motor. *Traffic* **2000**, *1*, 19−28.

(34) Das, D.; Das, D.; Padinhateeri, R. Collective Force Generated by Multiple Biofilaments can Exceed the Sum of Forces Due to Individual Ones. *New J. Phys.* **2014**, *16*, 063032.

(35) Janson, M. E.; de Dood, M. E.; Dogterom, M. Dynamic Instability of Microtubules Is Regulated by Force. *J. Cell Biol.* **2003**, *161*, 1029−1034.

(36) Padinhateeri, R.; Mallick, K.; Joanny, J. F.; Lacoste, D. Role of ATP-Hydrolysis in the Dynamics of a Single Actin Filament. *Biophys. J.* **2010**, *98*, 1418−1427.

DOI: 10.1021/acs.jpcb.5b01219
J. Phys. Chem. B 2015, 119, 4653−4661